The following supplements accompany the article

Connectivities with shellfish farms and channel rivers are associated with mortality risk in oysters

Aline Gangnery*, Julien Normand, Cyrielle Duval, Philippe Cugier, Karine Grangeré, Bruno Petton, Sébastien Petton, Francis Orvain, Fabrice Pernet

*Corresponding author: aline.gangnery@ifremer.fr

Aquaculture Environment Interactions 11: 493–506 (2019)

Supplement 1. Validation of the hydrobiological model for the year 2014

We used a 3-D hydrodynamic Model for Applications at Regional Scale (MARS-3D, Lazure & Dumas 2008) coupled with a biogeochemical model previously developed for the BdV (Grangere et al. 2010) to generate high frequency data (every hour) of seawater temperature, salinity, chlorophyll a concentration (derived from phytoplankton) and hydrodynamic connectivity to oyster farms and to the mouths of the channel rivers at the 39 sites. Seawater temperature and salinity were directly simulated by the hydrodynamic model and chlorophyll *a* derived from the biogeochemical model as the total quantity of nitrogen coming from diatoms, dinoflagellates and nano-pico-phytoplankton compartments. Nitrogen was converted into chlorophyll *a* concentration (µg l^{-1}) with a ratio varying with physiological status of phytoplankton and light environment (Ménesguen et al. 2019).

Values obtained from the model for each variable were compared with *in situ* measurements in the Baie des Veys. High-frequency records of seawater temperature and salinity were provided by the Ifremer oyster observatory network called RESCO at the sampling site Gefosse-RESCO, corresponding to site 39 (Fleury et al., 2015). This site was equipped autonomous temperature, pressure and salinity data logger (NKE Instrumentation, Hennebont, France). Simulated seawater temperature matched perfectly with observations ($r^2 = 0.99$, $p < 2.26 \times 10^{-16}$; Figure S1). Also, simulated salinity values were correlated with field observation ($r^2 = 0.45$, $p = 7.126 \times 10^{-16}$; Figure S1) but freshening events were not always well reproduced by the model.

Chlorophyll *a* concentrations were measured bimonthly from March to October and monthly for the rest of the year by the hydrological coastal monitoring network called RHLN (Menet-Nédélec et al. 2017). Two sampling sites were surveyed in the Baie des Veys: "Gefosse-RHLN", near site 21, and "Roches de Grandcamp" with the nearest corresponding site 33. Simulated values were globally within the range of field measurements (Figure S2) although the model overestimated at the end of the year (October-December 2014).

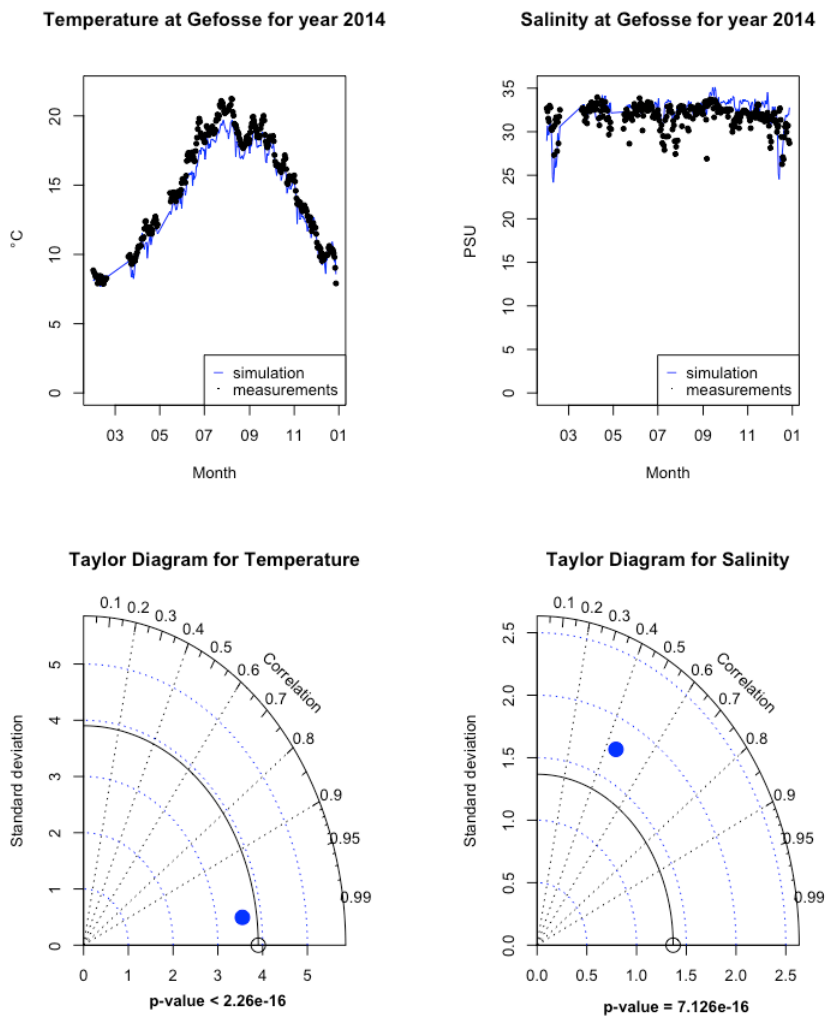

Figure S1: Mean daily variations of simulated (blue line) and measured (black circles) water temperature and salinity at site Gefosse-RESCO during the year 2014 (upper panel). For both parameters, Taylor diagrams presented a statistical evaluation of measurements-simulations similarity (lower panel). The black arc of a circle indicates the standard deviation of measurements and the projection of the blue circle on the correlation axis represents the correlation coefficient of the linear regression between measured and simulated data. The associated p-value was indicated under each graph.

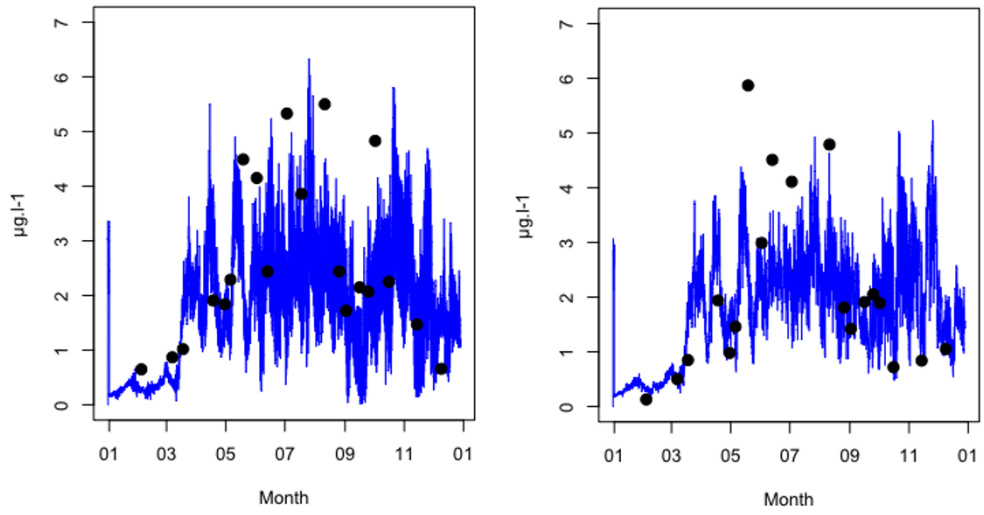

Figure S2: Temporal variations of simulated (blue line) and measured (black circles) chlorophyll *a* concentrations (µg l^{-1}) at Gefosse-RHLN (left) and Roches de Grandcamp (right) during the year 2014.

Supplement 2: Sampling sites connectivity with river channels and shellfish farming areas

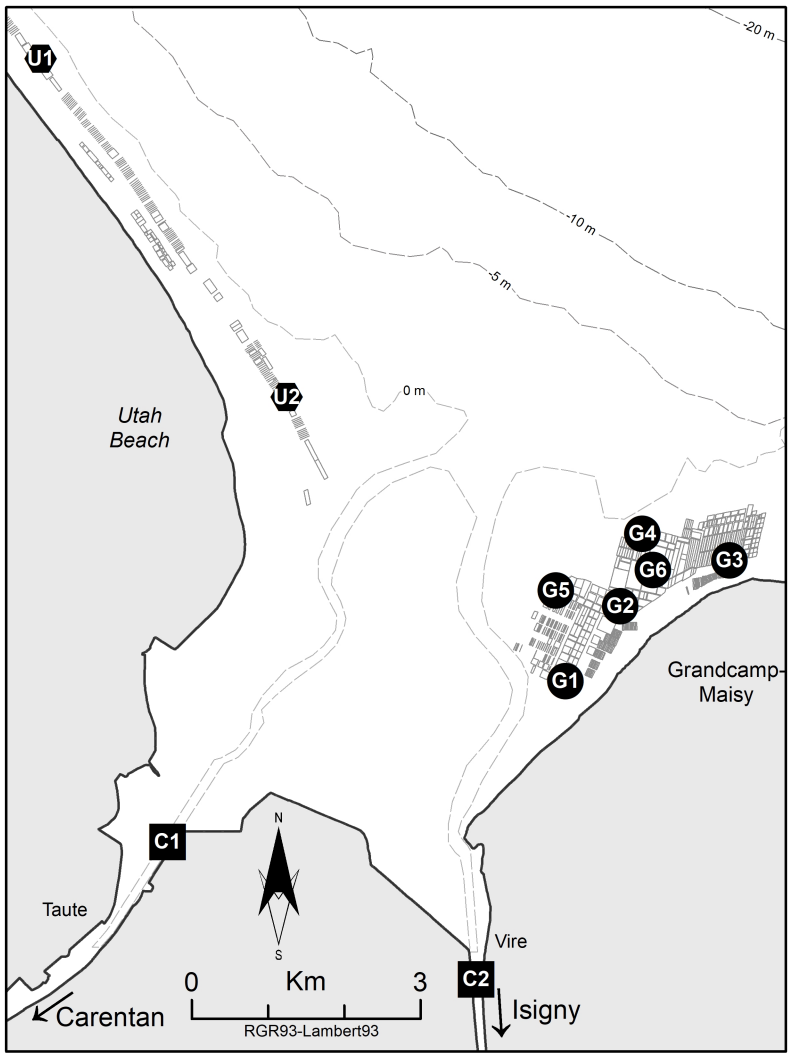

Figure S3: Locations of source sites used for connectivity estimations (C: Carentan and Isigny channels, G: Grandcamp farming area, U: Utah Beach farming area).

Table S1: Characteristics of simulations periods chosen for connectivity estimations. Douve and Taute flow through Carentan channel; Vire and Aure through Isigny channel.

Connectivity	**Dates of simulations**	**Tidal coefficient***	**Mean daily river inputs (m^3 s^{-1})**	**Winds (direction and force)**	**Oyster mortality**
To river channels	2014/01/29 - 2014/02/12	Min = 36 Max = 114	Douve = 25.29 Taute = 14.82 Vire = 66.64 Aure = 22.93	South – Southwest >5 knots	No
To farming areas for young oysters and adult oysters during period 1	2014/05/08 - 2014/05/19	Min = 38 Max = 97	Douve = 14.74 Taute = 4.61 Vire = 17.47 Aure = 0.02	West – Southwest <5 knots	Classically before juvenile mortality
To farming areas for adult oysters during period 2	2014/08/01 - 2014/08/15	Min = 44 Max = 113	Douve = 11.49 Taute = 1.59 Vire = 9.69 Aure = 0	West – Northeast <5 knots	Classically during adult mortality

* Tidal coefficient represents the amplitude of the tide forecast (difference in height between the consecutive high tides and low tides in any given area).

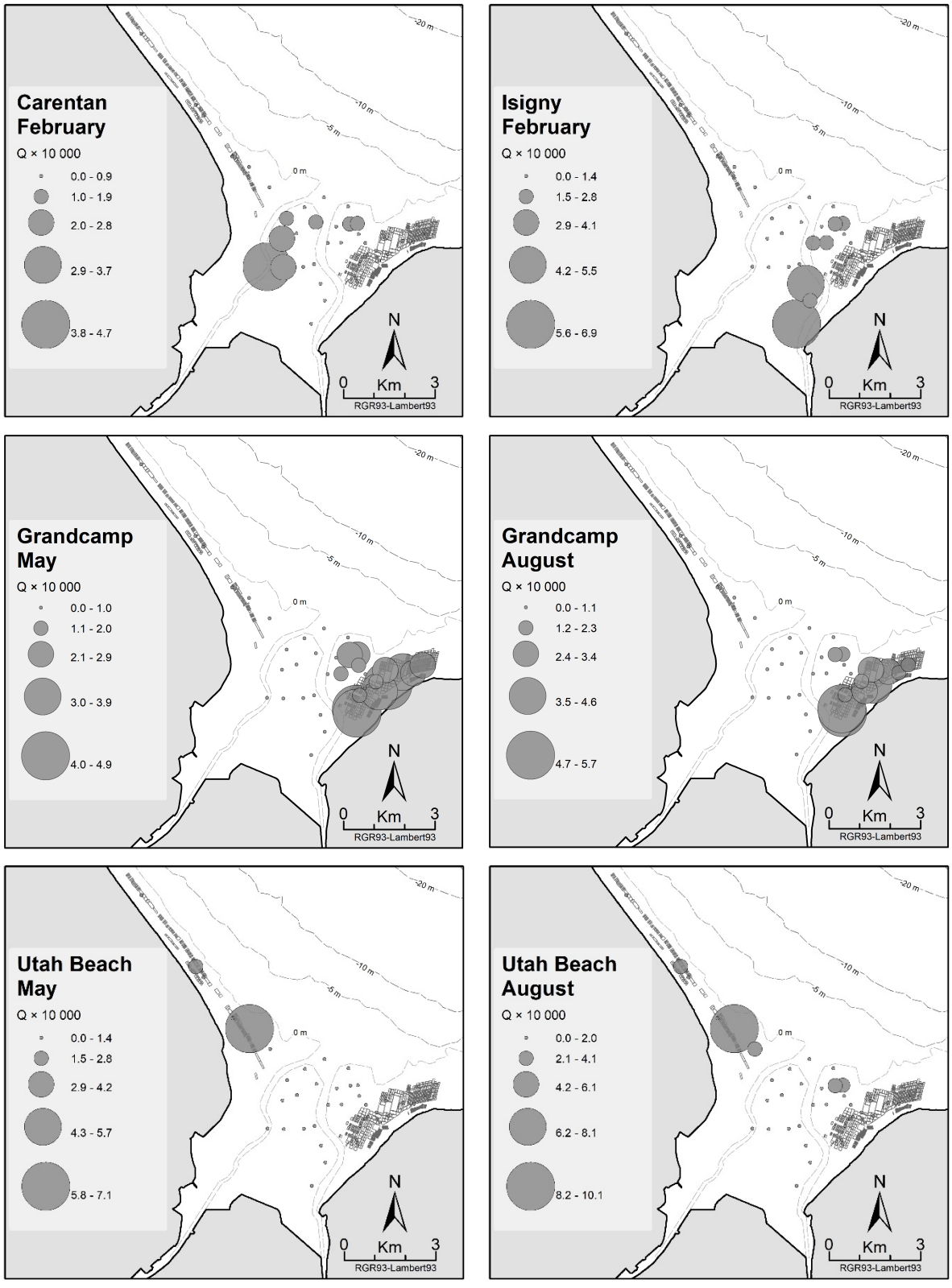

Figure S4: Maps of estimated connectivity for each sampling site and combination source type (Carentan and Isigny channels, Grandcamp and Utah Beach farming areas) and time period. For Grandcamp and Utah Beach farming areas, connectivity was averaged between source points.

Supplement 3: Smoothing procedure applied to young oysters

At each sampling date and site, the mortality proportion of young oysters was estimated on a sub-sample of the overall population contained in each bag.

The cumulative proportion of mortality over time was calculated as follows:

$$P_t = \frac{\mathrm{Nd}_t}{\mathrm{Nd}_t + \mathrm{Na}_t}$$

where Nd_t is the number of dead oysters and Na_t the number of alive oysters at day t.

Because of sub-sampling, proportion of mortality did not increase monotonically in the majority of cases. We therefore applied a smoothing procedure to re estimate mortality data at each date and sampling site. According to the previous studies of OsHV-1-associated young mortalities, all the authors reported that time-mortality curves presented a sigmoid shape in the field as well as in controlled conditions (Petton et al. 2013, Pernet et al. 2014).

Therefore, a sigmoid curve was fitted to the data using the following equation:

$$P_t = \frac{\mathrm{a}}{1+exp^{-b\times(t-c)}}$$

where P_t is the proportion of dead oysters at time *t*, expressed in julian days, from the beginning of the experiment and *a*, *b*, and *c* represent the parameters of the sigmoid to be adjusted.

The BGFS (Broyden-Fletcher-Goldfarb-Shanno) optimization procedure, based on quasi-Newton method, was used to estimate each set of a, b and c parameters at each sampling site (Nash, 2014) (Figure S5). Predicted mortality proportions were then extracted at each sampling date to reconstruct discrete mortality curves. For young oysters, data analysis focused on the final cumulative mortality proportion. We therefore used these final predicted values and regressed them against observations to assess the quality of smoothing (Figure S6).

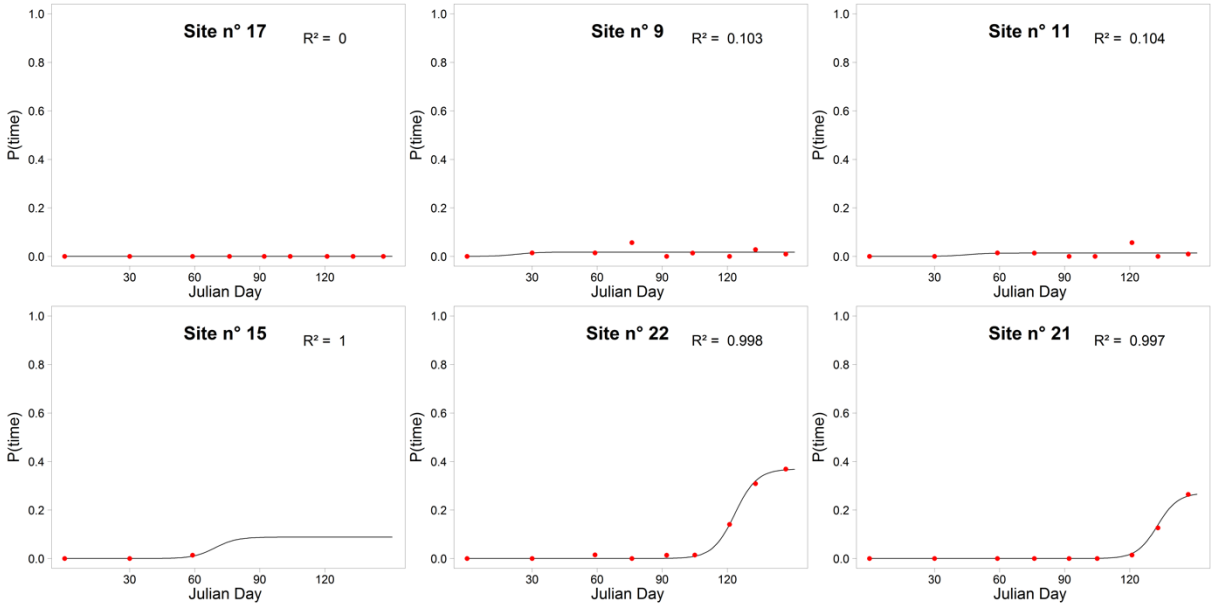

Figure S5: Adjustment of sigmoid models (black curve) on mortality observations (red points). Graphs on the upper panel correspond to sampling sites with the lowest R^2 values whereas graphs on the lower panel correspond to sampling sites with the highest R^2 values.

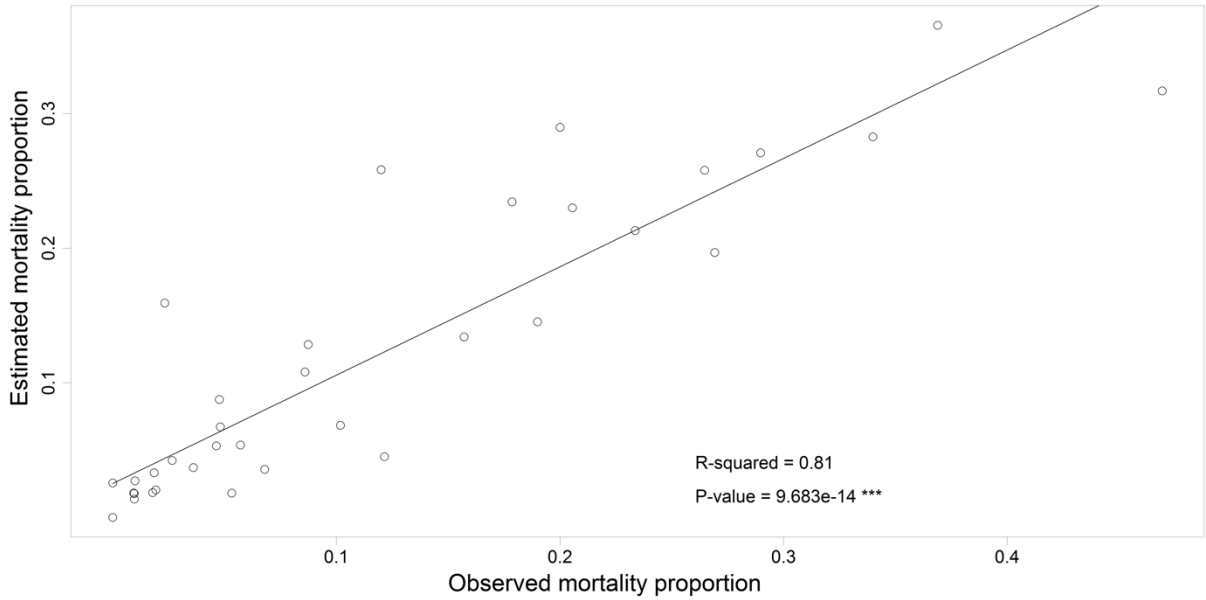

Figure S6: Estimated mortality proportions at the end of the survey regressed against observed mortality proportions. The R-squared value and the p-value associated with Fisher test are reported on the graph.

Supplement 4: Simple variograms of oyster mortality

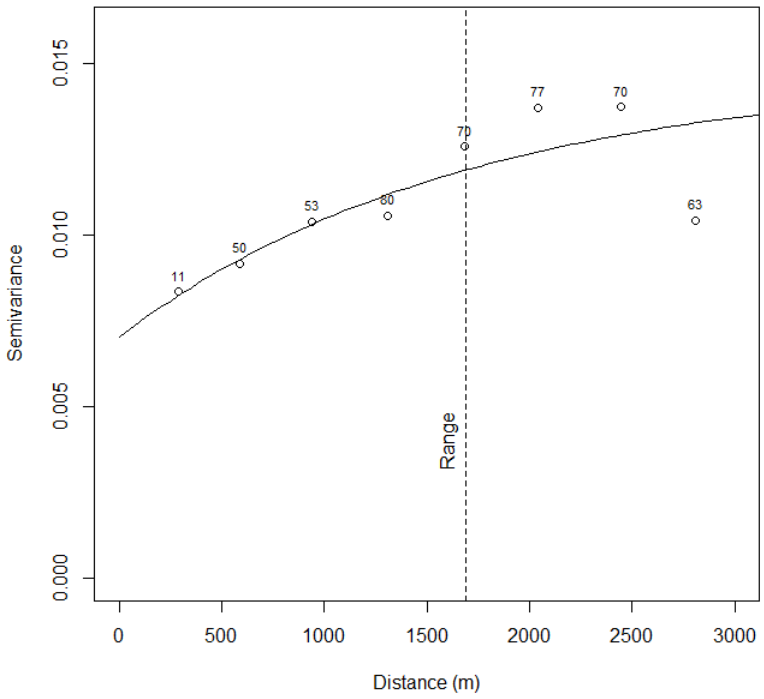

Figure S7: Variogram of young oyster mortality. Numbers indicate for each distance class the number of pair of sites.

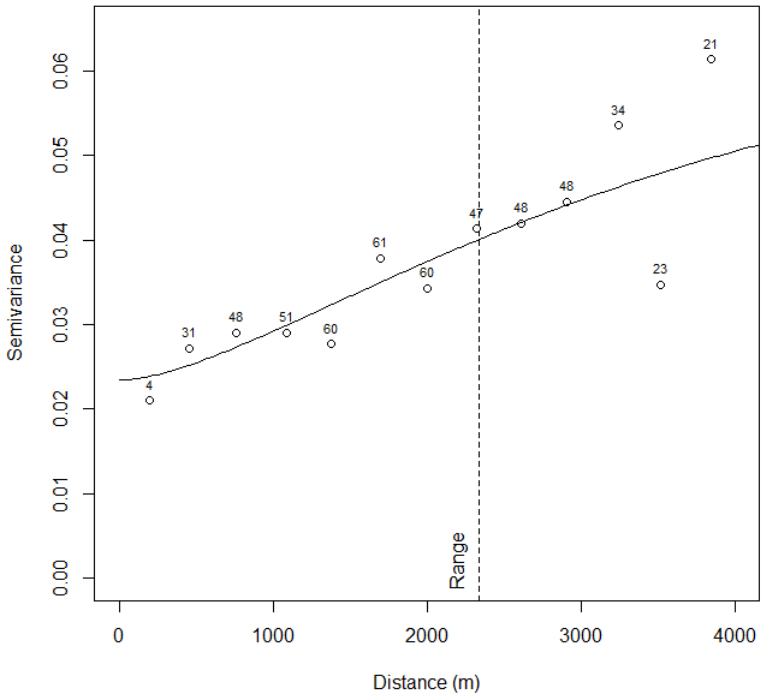

Figure S8: Variogram of adult oyster mortality during period 1. Numbers indicate for each distance class the number of pair of sites.

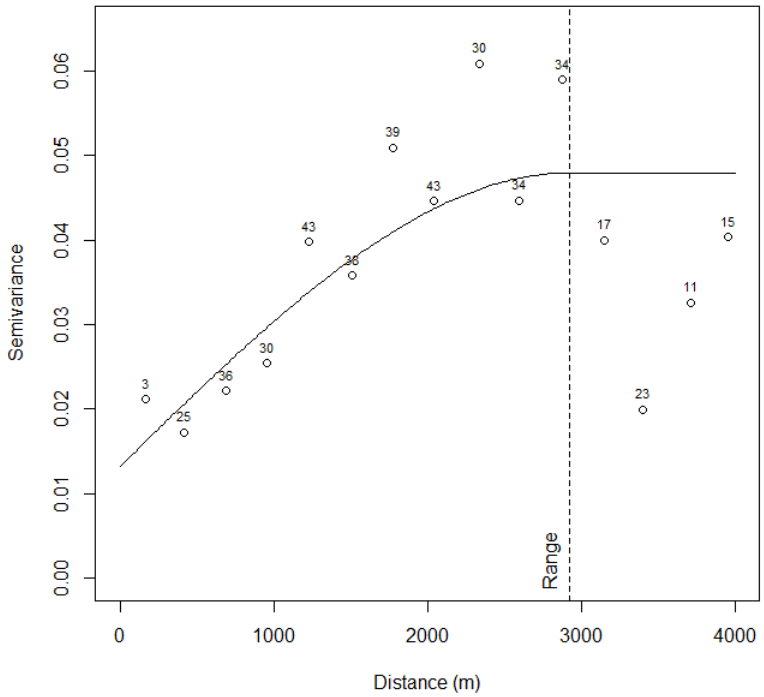

Figure S9: Variogram of adult oyster mortality during period 2. Numbers indicate for each distance class the number of pair of sites.

Supplement 5: Logistic regression between the cumulative mortality of young oysters and the proportion of individuals infected with OsHV-1 in June

A logistic regression model was fitted between the cumulative mortality simulated in June 30 and the proportion of individuals infected with OsHV-1 in June 13-16.

Coefficients of the logistic regression model:

	Estimate	Std. Error
(Intercept)	-6.597	1.270
Proportion of infected oysters	5.408	1.305

Results of Chi square test:

	Df	Deviance	Resid. Df	Resid. Dev	Pr(>Chi)
NULL			11	1.99305	
Prop. of infected oysters	1	1.7603	10	0.23277	**4.905×10^{-16}** ***

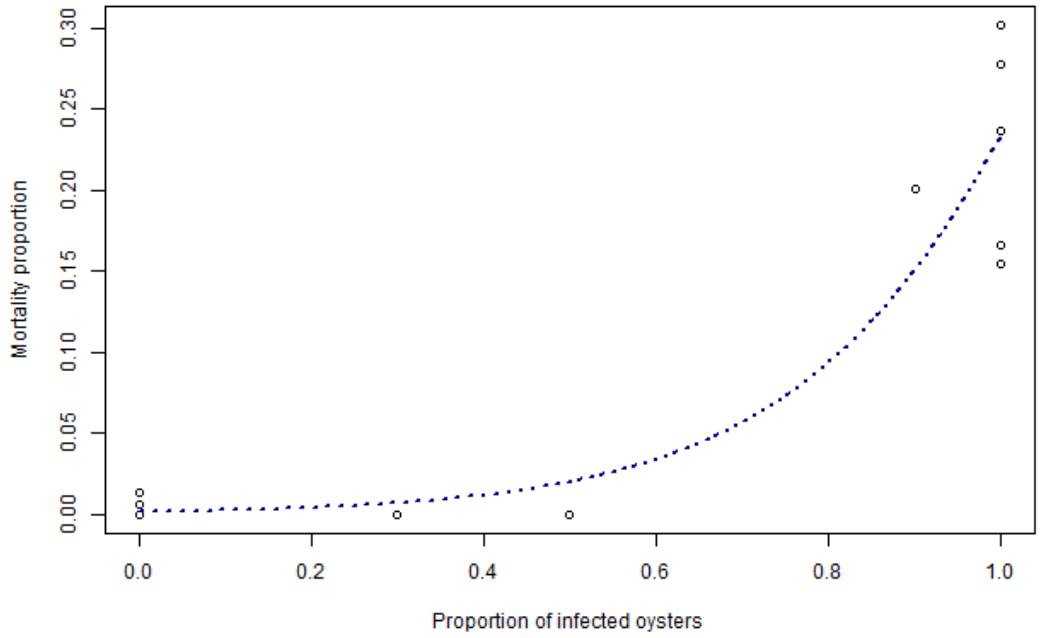

Figure S10: Young oyster cumulative mortality as a function of proportion of infected individuals and predictions by the logistic regression model (n=12 sites).

Supplement 6: Maps of environmental variables used for mortality predictions by co-kriging

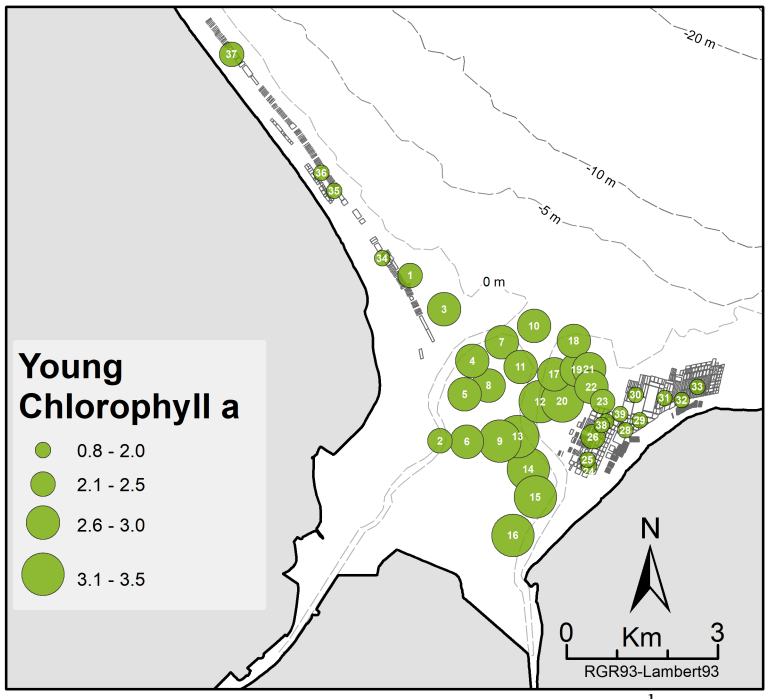

Figure S11: Map of estimated chlorophyll a concentration (µg.l^{-1}) during the whole period and used for predictions of young oyster mortality.

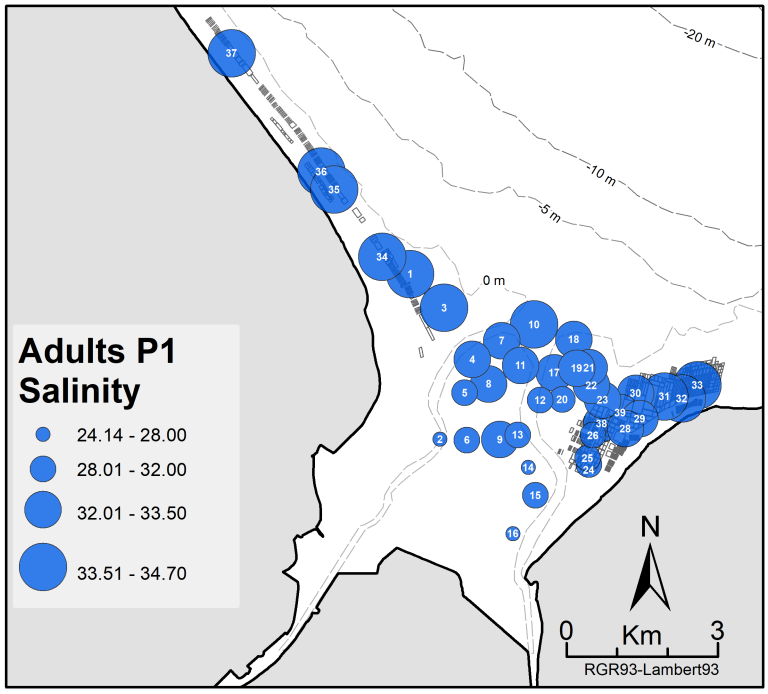

Figure S12: Map of estimated salinity during period 1 and used for predictions of adult oyster mortality.

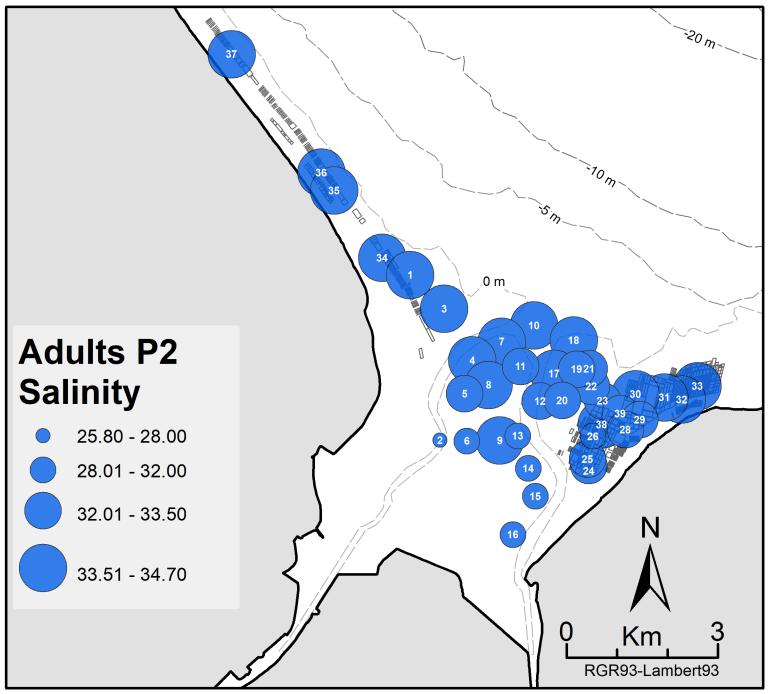

Figure S13: Map of simulated salinity during period 2 and used for predictions of adult oyster mortality.

References

Grangere K, Lefebvre S, Bacher C, Cugier P, Menesguen A (2010) Modelling the spatial heterogeneity of ecological processes in an intertidal estuarine bay: dynamic interactions between bivalves and phytoplankton. Mar Ecol Prog Ser 415:141-158

Lazure P, Dumas F (2008) An external-internal mode coupling for a 3D hydrodynamical model for applications at regional scale (MARS). Adv Water Resour 31:233-250

Ménesguen A, Dussauze M, Dumas F, Thouvenin B, Garnier V, Lecornu F, Répécaud M (2019) Ecological model of the Bay of Biscay and English Channel shelf for environmental status assessment part1: Nutrients, phytoplankton and oxygen. Ocean Model 133:56-78

Menet-Nédélec F, Ropert M, Riou P, Courtay G, Fontaine B, Françoise S, Jacqueline F, Lesaulnier N, Louis F, Maheux F, Pierre-Duplessix O, Rabiller E, Schapira M, Simon B (2017) Réseau Hydrologique Littoral Normand, Année 2014. Rapport Ifremer ODE/LERN/17-07

Nash JC (2014) On Best Practice Optimization Methods in R. Journal Stat Softw 60:2

Pernet F, Lagarde F, Jeannée N, Daigle G, Barret J, Le Gall P, Quéré C, Roque D'orbcastel E (2014) Spatial and temporal dynamics of of Mass Mortalities in Oysters is influenced by energetic reserves and food quality. PlosOne 9:e88469

Petton B, Pernet F, Robert R, Boudry P (2013) Temperature influence on pathogen transmission and subsequent mortalities in juvenile Pacific oysters *Crassostrea gigas*. Aquaculture Env Interact 3:257-273